Time-resolved electron beam fluorescence for measuring neutral particles in EP plasmas

IEPC-2017-30

Presented at the 35^{th} International Electric Propulsion Conference, Georgia Institute of Technology, Atlanta, Georgia, USA
October 8–12, 2017

Curtis L. Promislow,[*] Anna J. Sheppard[†]
University of Washington, Seattle, WA, 98105, USA

Justin M. Little[‡]
MSNW LLC, Redmond, WA, 98052, USA
University of Washington, Seattle, WA, 98105, USA

Abstract: A proof-of-concept time-resolved electron beam fluorescence diagnostic has been fabricated to determine the feasibility of measuring the density of neutral particles near operating electric thrusters. Such a measurement capability would be valuable in obtaining a deeper understanding of mass utilization in pulsed electromagnetic thrusters, and the role of facility background pressure on the evaluation of thruster performance in a ground test environment. Using a wire induced plasma source and secondary electron emission through ion bombardment of an aluminum cathode, a ∼100 μA, 20 kV beam was generated with a beam waist of ∼5 mm. Measurements of the visible emission from a pulsed plasma source suggest a temporal resolution of ∼1 μs for the fluorescence detection system. By measuring the fluorescence intensity resulting from excitation of a background gas by the electron beam, neutral densities as low as 6×10^{19} m^{-3} were detected. Methods for order of magnitude increases in neutral resolution are discussed along with potential limitations of the diagnostic for EP testing and evaluation.

I. Introduction

A need exists within the EP community for a diagnostic that can resolve the spatial and temporal features of the neutral gas in the vicinity of operating electric propulsion (EP) thrusters. Such measurements are critical for predictive plasma models, analysis of modern testing and evaluation capabilities, and the development of next generation thrusters. Investigated here is one such possibility, electron beam fluorescence, that uses an electron beam to excite neutral particles, which can then be characterized via the resulting fluorescent radiation.

There exist relatively few neutral gas diagnostics in the literature for partially-ionized, non-equilibrium plasmas. Walker and Gallimore[1] used an array of five fast-ion gauges to map the neutral density profile in the downstream region of an operating 5 kW Hall thruster. The large dimensions of the probe (10 cm) used in this study limit its spatial resolution to a few centimeters and preclude its use near the operating thruster. Crintea et. al.[2] combined optical emission spectroscopy (OES) with Thomson scattering (TS) and a collisional-radiative model (CRM) to measure the density of different excited neutral states in an inductively coupled plasma down to very low densities (∼10^{15} m^{-3}). The use of a CRM required an accurate measurement of the electron temperature, necessitating TS, and limiting the temporal resolution of the measurements. Hori et. al.[3] measured the scattering of a Nd:YAG laser from an inductively coupled plasma source and determined the neutral gas density from the Rayleigh scattered signal, however, their

[*]Graduate Student, Department of Aeronuatics and Astronautics
[†]Graduate Student, Department of Aeronautics and Astronautics
[‡]Principal Investigator, Research Scientist, Department of Aeronautics and Astronautics

measurements required long acquisition times ($\sim 10^2$ s) and were limited to relatively high densities ($\sim 10^{20}$ m^{-3}). The first measurements of the spatially-resolved neutral xenon density in an operating Hall thruster were made by Crofton et. al.[4] using two-photon laser induced fluorescence (2PLIF). The large band-gap between the neutral xenon ground state and first excited states is not directly accessible with existing laser technology and necessitates the use of two-photon excitation. Using this technique the authors were able to spatially resolve ($\sim$1 mm) xenon neutral densities on the order of $\sim 10^{18}$ m^{-3}. A similar system was used by Aanesland et. al. to measure neutral density depletion in a helicon plasma.[5] The extension of the technique to time-resolved measurements was not investigated in detail, although previous use of the diagnostic would suggest temporal resolutions of a few hundred microseconds.[6]

The Time-Resolved Electron Beam Fluorescence (TREBF) system presented here non-invasively probes neutral gas dynamics on length ($\sim$1 mm) and time ($\sim 1\,\mu$s) scales relevant to EP plasmas. The technique relies on the interaction of an electron beam with the plasma neutral particles. The beam creates a population of excited atomic or molecular neutral particles through electron impact excitation (pumping). Photons emitted via radiative de-excitation (fluorescence) are selectively sampled to reveal the neutral gas composition, density, and energy distribution. EBF has a long heritage in the investigation of low-density (10^{19}-10^{22} particles/m^3) hypersonic flows.[7] The technique has been used within the EP community to study low-power (weakly ionized) arcjet[8] and cold gas thruster plumes[9] and the distribution of neutral gas injection in non-operating Hall thrusters.[10]

This paper will focus on the design and testing of a proof of concept experiment to demonstrate the efficacy of TREBF towards diagnosing neutral particle flow dynamics in non-equilibrium, partially-ionized EP plasmas. We will describe the development of a compact, low-cost electron gun, detection optics, and high-speed gated PMT. Vacuum testing of the diagnostic was performed to measure the diagnostic accuracy and density, temporal and spatial resolutions.

II. Motivation, Background, and Theory

A. Pulsed Thruster Mass Utilization

The mass utilization efficiency of an electric thruster refers to the fraction of input propellant that contributes to the thrust of the device. Propellant use inefficiencies oftentimes result from incomplete ionization of incoming propellant gas, which then exits the thruster at near-thermal velocities. This can been especially problematic for pulsed devices such as the Pulsed Inductive Thruster (PIT)[11] and Field-Reversed Configuration (FRC),[12] which rapidly form and electromagnetically accelerate high-density plasmoids. The propellant distribution prior to a pulse not only influences the formation of the plasma currents but also the entrainment and acceleration of propellant downstream from the region of formation. It is the these entrainment and acceleration processes that are key to mass utilization in devices where the pulse period is on the order of, or greater than, the transit time of the neutral propellant gas through the thruster. Understanding the neutral transit time and propellant distribution in between pulses is a critical challenge in improving the efficiencies of these devices.

B. Facility Effects

Facility effects broadly refer to the disparity in performance of EP devices in vacuum chambers compared to other vacuum chamber experiments and on-orbit data. Thrust and specific impulse values derived from telemetry data[13,14] have shown reasonable agreement with test chamber measurements; however, uncertainties associated with this method can be quite large.

Randolph et. al.[15] performed early research in support of the adoption of the SPT-100 Hall thruster for US satellites and proposed a number of facility criteria for reliable T&E of this specific device. A few conclusions can be drawn from this study: (1) the background neutrals affect a variety of physical phenomenon that influence thruster operation, stability, and lifetime; (2) the thruster age influences operation and the manner in which it interacts with the facility neutrals, and (3) the dependence of thruster performance with background pressure shows poor agreement among different facilities. Byers and Dankanich[13] reviewed the background pressure effects on Hall thruster tests that spanned a period of over two decades. They argue that the effect of background pressure on the operating thruster cannot be corrected using a semi-empirical neutral ingestion model, and that the physical interaction of facility neutrals with the thruster plasma is more complex than originally anticipated. The situational nature of the background pressure effect on Hall thruster testing was shown in great detail by Brown and Gallimore,[16] which demonstrate the complexity of the facility effects problem in the following ways: (1) even a small excess of neutral particles can have a large impact on the nature of the plasma oscillations in the thruster, (2) the oscillations themselves can drive large-scale changes in thruster operation, and (3) different operating modes can exhibit vastly different performance numbers. A recent study by Diamant, Liang, and Corey[14] examined in detail the role of the background pressure at two different facilities on the measured performance, plume properties, and operating characteristics of an SPT-100 Hall thruster, and observed the following trends with increasing background pressure: (1) increased thrust, efficiency, and specific impulse, (2) decreased total flow rate to maintain constant power, (3) increased thruster oscillations, (4) increased number of low energy ions in the plume, and (5) decreased plume divergence angle. Furthermore, they also show that the ingestion model is insufficient to explain their observations, and echo the sentiment that a deeper fundamental understanding of the interaction of the plasma with the background neutrals is required to explain the pressure sensitivity.

In general, the literature indicates that the present model for ingestion of the facility neutrals is insufficient to explain the complex phenomenon observed of Hall thrusters operating at different background pressures. These findings can be extrapolated to other EP devices, although the exact extent of facility effects on different thruster architectures remains to be studied. A detailed study of the influence of facility effects on a broader class of thrusters using state-of-the-art diagnostics will be crucial to the understanding of thruster T&E at higher powers and the refinement of thruster plume-spacecraft interaction models.

C. Time-Resolved Electron Beam Fluorescence

Time-Resolved Electron Beam Fluoresence (TREBF) is a neutral particle diagnosic that promises to significantly enhance EP T&E and predictive modelling capabilities by probing neutral particle dynamics on time and length scales relevant to non-equilibrium, partially-ionized EP plasmas. The TREBF diagnostic system, shown schematically in 1, consists of an electron gun, beam deflector, collection optics, optical filter, and photodetector.

When an electron from the beam collides inelastically with a neutral atom or molecule, part of the kinetic energy of the electron is converted into internal energy of the atom, causing it to transition into an excited state. If this excess internal energy is not lost due to collision with another molecule or atom within the lifetime of the excited state, a process sometimes referred to as non-radiative collisional quenching,[17] it is instead shed via the emission of a photon, i.e., via fluorescence. The fraction of excited atoms which decay due to collisional de-excitation versus fluorescence is, perhaps unsurprisingly, a function of the gas density, ρ (or equivalently n).[17] The exact nature of the dependence, however, depends itself on the density of the gas. Following Gadamer,[17] the intensity of the fluoresced light, I_f, may be written in terms of the total energy

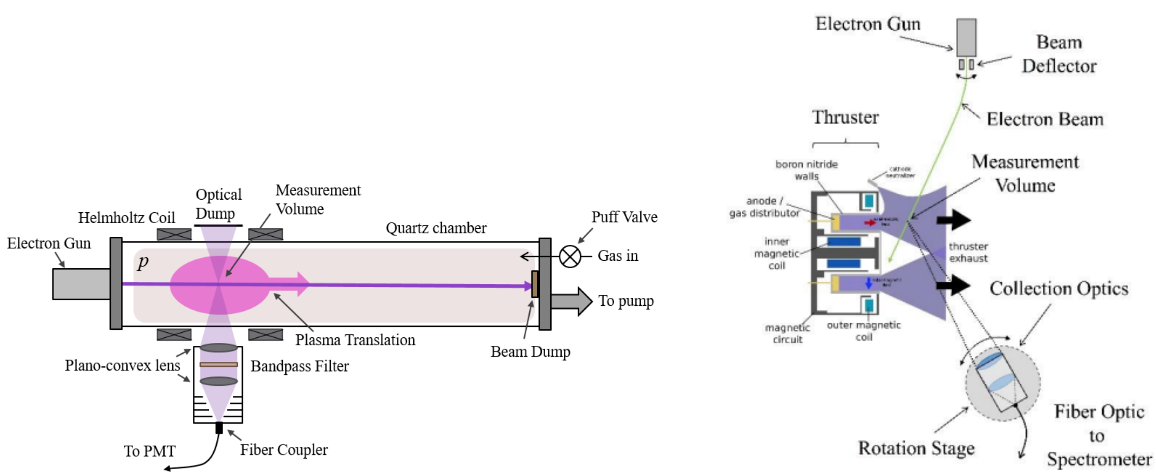

(a) Proof of concept **(b) In practice**

Figure 1. (a) Initial characterization, as more fully described in this paper, was conducted using this proof of concept experimental set-up. (b) The TREBF system can be used to interrogate EP plumes, such as those from a Hall thruster, as shown here.

deposited into the neutral molecules via inelastic collisions with beam electrons, W, and the fluorescent light yield, Φ:

$$I_f = W\Phi \tag{1}$$

While it has been found that W is directly proportional to ρ over a wide range of gas densities, the relationship between Φ and ρ is, in general, less straightforward. At the low gas densities relevant to EP thrusters ($\lesssim 1\,\mathrm{Torr}$), however, the number of molecules that experience non-radiative collisional de-excitation is low, which necessitates that a majority of the excited molecules decay via fluorescence. As a result, Φ becomes insensitive to density and I_f is found to scale linearly with ρ,[17]

$$I_f \sim \rho\Phi\,, \tag{2}$$

where Φ is now a constant with respect to pressure. Since pressures in most EP relevant applications are typically on the order of a few tens of mTorr or less, it is expected that the intensity of the fluoresced light will scale linearly with the gas pressure over a wide range of applications.

III. Experimental Design

A. Electron Gun

A secondary emission electron gun was developed following the design of Diop et al,[7] which has been successfully used in investigating hypersonic flows. A wire induced plasma source (WIPS) generates ions which are accelerated towards a cathode held at high potential (on the order of several to 10s of kV). The ions impinging on the cathode release secondary electrons which are passively collimated by an aperture restricting the divergence of the beam and actively collimated by magnetic fields. A schematic can be found in Fig. 2. This secondary emission is independent of the background pressure of the facility, and a separate gas source feeds the plasma within the gun. Facility effects can thus be studied without correcting for the intensity of the electrons entering the region of interest, as described in section II.B.

To drive down the cost of the diagnostic, the electron gun is housed in a series of standardized $2\,{}^3\!/_4$ ConFlat® fittings. Blank copper gaskets serve as the interfaces between sections of the gun and were turned on a lathe to ensure alignment of orifices. Differential pumping of the gun using a small turbopump is required to ensure pressure near the cathode is held below that required for Paschen breakdown. Aluminum was chosen as the cathode material because of its relatively high secondary electron yield.[7] After a few hours of operation, a small pit ($\sim 1\,\mathrm{mm}$ in both diameter and depth) developed, consistent with the results reported by Diop et al. The WIPS, which doubled as the anode of the gun, consists of a thin tungsten wire ($D = 0.01\,\mathrm{in}$) attached to a high voltage ($5\,\mathrm{kV}$ and $60\,\mathrm{mA}$) power supply. The supply is used to both create

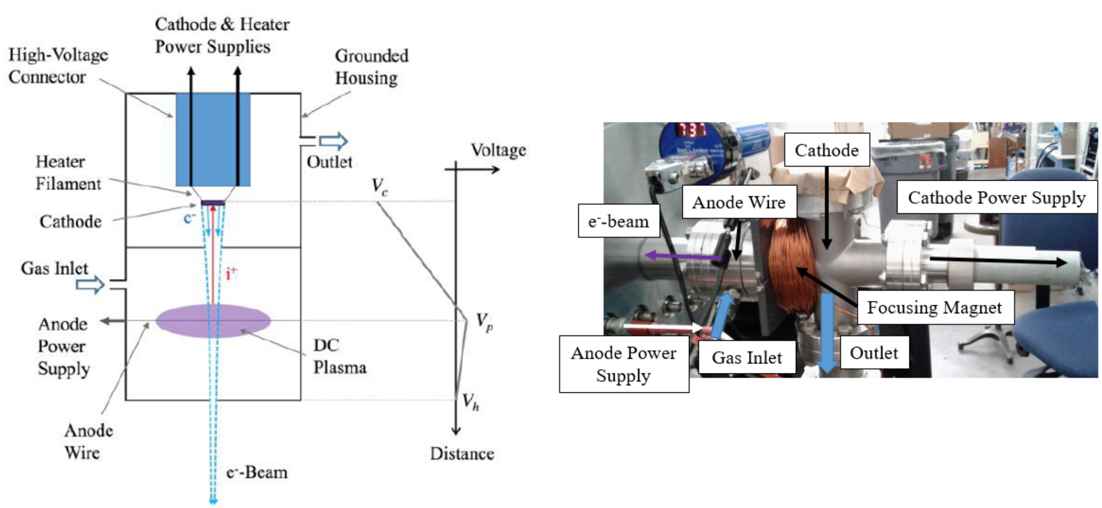

Figure 2. Schematic of secondary emission electron gun, centerline voltage profile, and assembled electron gun.

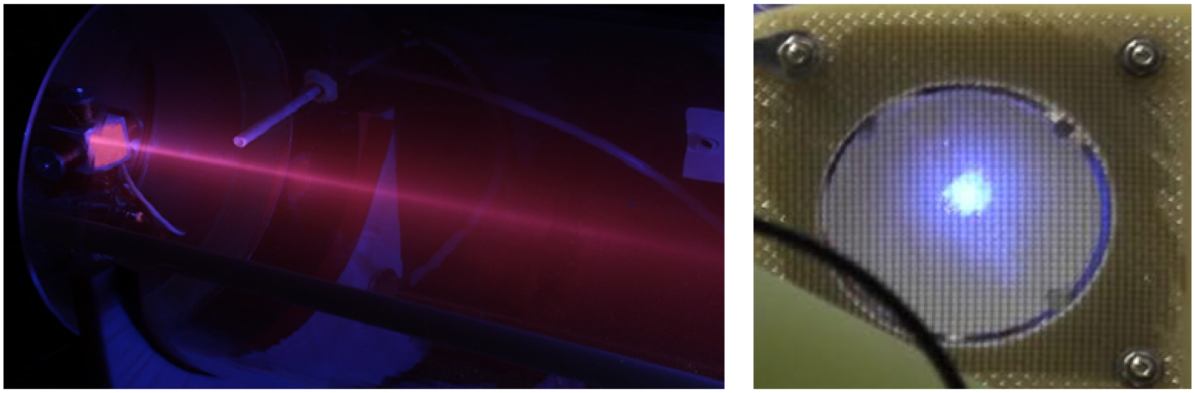

(a) Electron beam **(b) Phosphor screen**

Figure 3. (a) In neon, the electron beam produced by the electron gun on the left hand side of the photo. (b) A phosphor screen is illuminated to show the spatial spread of the electron beam. Each square of the mesh is approximately 1 mm on a side.

the voltage necessary for gas breakdown and control the current supplied to the WIPS. By controlling the WIPS current, the ion fluence to the cathode, and therefore the rate of secondary electron emission, can be adjusted. A WIPS current of 3 mA was found to be optimal for stability of the gun. Gas breakdown in the gun is reliably achieved by applying 1 - 2 kV to the anode when the pressure in the gun is above ≈ 50 mTorr. After breakdown, the WIPS can be sustained at pressures of $\sim$20 mTorr or higher.

The electron beam produced can be seen at sufficiently high pressures ($\sim$ 100 mTorr), as shown in Fig. 3. A grid with $\sim$1 mm grid spacing was backlit by a phosphor screen to determine beam diameter; in Fig. 3, the beam diameter is approximately $\sim$6 mm. The phosphor screen works across a wider range of pressure compared to the human eye, and care must be taken to not damage the surface with too much incident power. Beam diameter estimates were taken separately from fluorescence measurements in order to mitigate the effect of the screen's perturbation and fluorescence on collected data. The beam diameter did not appear to vary with cathode voltage but could be modified with magnetic lenses. A focusing magnet was used to vary the focal point of the electron beam over a $\sim$50 cm range, and narrow the beam waist. While smaller diameter beams could be obtained, ultimately this magnet was not used during neutral density measurements due to variability at different pressures. Further, deflection magnets from a cathode ray tube television were installed to steer the beam. Deflection angles up to 90 deg are attainable, and this deflection could be used to determine the energy distribution of the beam in conjunction with a Faraday cup. This was not attempted for this experiment, as the measurement sensitivity was insufficiently high. However, a Faraday cup was constructed to determine the total beam current, and measurements indicated that the beam is at most 10% of the cathode current. Charging of the Faraday cup appeared to be an issue, and alternative methods of determining beam current were explored, including those mentioned by Diop et al.[7] Further characterizations of the beam were not attempted, however, as the performance met the requirements necessary to pursue evaluating TREBF's feasibility in determining neutral density in EP plasmas.

B. Optics and Fluorescence Detection

Light emission was collected using a fiber collimator positioned approximately 25 cm downstream of the exit of the electron gun and oriented perpendicular to the direction of beam propagation. A fiber collimating lens was used to enable a wider field of view and improve the sensitivity of the measurement system. Due to the relatively weak emissions output expected at EP relevant pressures (typically no more than a few mTorr), a photomultiplier tube (PMT) was used to amplify the signal to measurable levels. The PMT (Thorlabs PMTSS) used was of the side-on, multialkali type and a spectral range of between 185 nm to 900 nm. The PMT had a recommended gain range of 3×10^2 to 4×10^6, which allowed for sufficient amplification of the emissions across a wide range of experimental conditions.

C. Plasma Source

A pulsed plasma source based on an inductive theta pinch design was constructed to assess the ability of the proposed diagnostic to perform neutral particle measurements in an EP relevant plasma environment. Specifically, a series of inductive coils was used to generate and expel a field reversed configuration (FRC) plasmoid from the quartz test section of the chamber. It has been theorized that an FRC pushes most of the background gas in the chamber along with it as it moves. If true, there should be some period over which the neutral population in the FRC formation section becomes depleted and then recovers to its background level over some refill timescale. By gating the PMT, it is possible for the TREBF diagnostic to measure the neutral particle density immediately following the FRC formation and ejection, thus providing the refill time of the neutral particles.

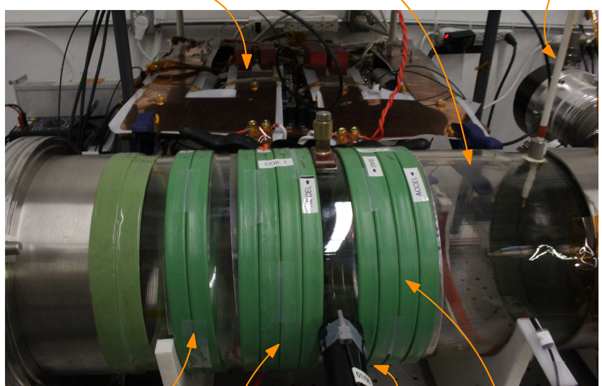

Figure 4. EBF chamber with inductive coils for plasma generation.

The major components of the source are shown installed on the TREBF vacuum chamber in Fig. 4. The two main antenna coils (coil 1 and 2), each consisting of a pair of two turns of flat copper braid connected in series, are responsible for FRC formation and ejection while the third trim coil (a single two turn coil) is used to prevent excessive magnetic flux loss during the formation process. A surface discharge sparker provides a source of seed electrons to help initiate gas breakdown. For these tests, the collection lens for the PMT was positioned directly between coils 1 and 2, as shown in Fig. 4.

The FRC was formed using a slight variation of the standard inductive theta pinch formation method, commonly described in the literature.[18] First, a bias magnetic field is generated in the chamber by running current through all three antennas while, at the same time, seed electrons are introduced by the sparker. Next, the coils are operated as a ringing theta pinch to pre-ionize the gas in the chamber. Finally, the accelerator bank is fired, driving current in the coil in the opposite direction to the bias bank. This causes a reversal of the magnetic field inside chamber and forms the FRC. Unlike the FRC formation techniques used in fusion experiments, however, the accelerator current is allowed to ring for a full cycle, rather than being crowbarred after the first half cycle. This causes the FRC to be accelerated and ejected from the chamber test section at high velocity.

Table 1. Important circuit parameters of bias, ringing theta, and accelerator PPUs.

	C (μF)	f (kHz)	T (μs)	L (μH)	V_{max} (V)	I_{max} (kA)	E (J)
Bias	160.0	6.6	151.5	3.63	300	1.99	7.20
Theta	1.3	140.0	7.1	0.98	1500	1.74	1.49
Accel	66.0	19.7	50.8	0.99	550	4.49	9.98

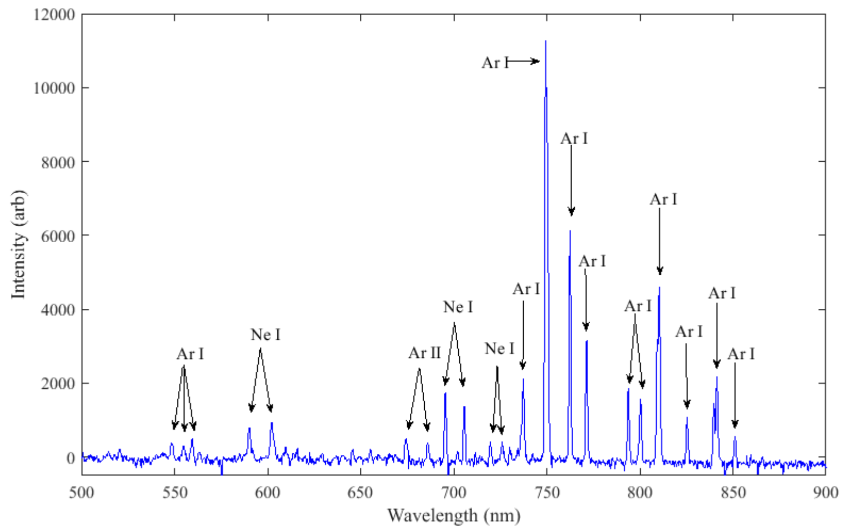

Figure 5. Spectrum generated by neutral atoms excited by EBF. Some neon contamination from previous testing is indicated by the presence of several Ne I lines. This data was collected from a 30 s long exposure at approximately 100 mTorr and background subtracted.

IV. Experimental Characterization

A. Measurement of the Fluorescence Spectrum

To gain a better understanding of which neutral species were being excited by the electron beam, collected light was transmitted via a fiber optic cable to an Ocean Optics spectrometer with a spectral range of 200 nm to 1100 nm. A representative spectrum can be seen in Fig. 5. While most of the emissions are from excited neutral argon fluorescence, light from excited neon and singly ionized argon was also present in small quantities. The detection of singly ionized argon is to be expected, since the energy of the electrons in the beam (on the order of several to tens of keV) should be more than sufficient to cause collisional ionization of the neutral gas. The detection of Ne I lines, however, indicates some degree of neon contamination in the chamber, likely resulting from preliminary experiments examining the beam behavior in various gases, as shown in Fig. 3a.

B. Neutral Density Measurements and Diagnostic Resolution

Before proceeding to EP relevant applications, it was first necessary to determine how the intensity of the measured emissions was affected by key experimental parameters, namely the pressure in the vacuum chamber and electron gun, as well as the voltage applied to the cathode. To this end, the total emission intensity was measured over a range of chamber background pressures while the gun pressure and cathode voltage were systematically varied. In addition, the emissions measured both with and without a colored glass longpass filter (725 nm, Schott RG9) were compared to determine if the intensity of fluoresced light followed similar trends to the total intensity of all light emissions. For the tests described in this section, the operating conditions on the electron gun were fixed while pressure in the quartz test section was varied by changing the flow rate of argon into the chamber. No measurements were taken until the pressure had equilibrated. The gain on the PMT was set to the highest recommended value ($\approx 4 \times 10^6$) to maximize the sensitivity of the detection scheme. The photocurrent produced by the PMT was converted to a measurable voltage by passing the PMT output directly through the 1 MΩ input of an oscilloscope. Since the PMT module and coaxial transmission cables were estimated to have a combined parallel capacitance of roughly 50 pF, the time response of the measurement system was thought to be on the order of $t_{RC} = (1\,\mathrm{M\Omega}) \cdot (50\,\mathrm{pF}) = 50\,\mu\mathrm{s}$, which was considered acceptable for the steady state measurements taken here. The signal intensity was measured over a 100 ms window and then temporally averaged to mitigate the effects of any transients. The average of 10 such temporal averages was then taken as the signal intensity for a given set of parameters.

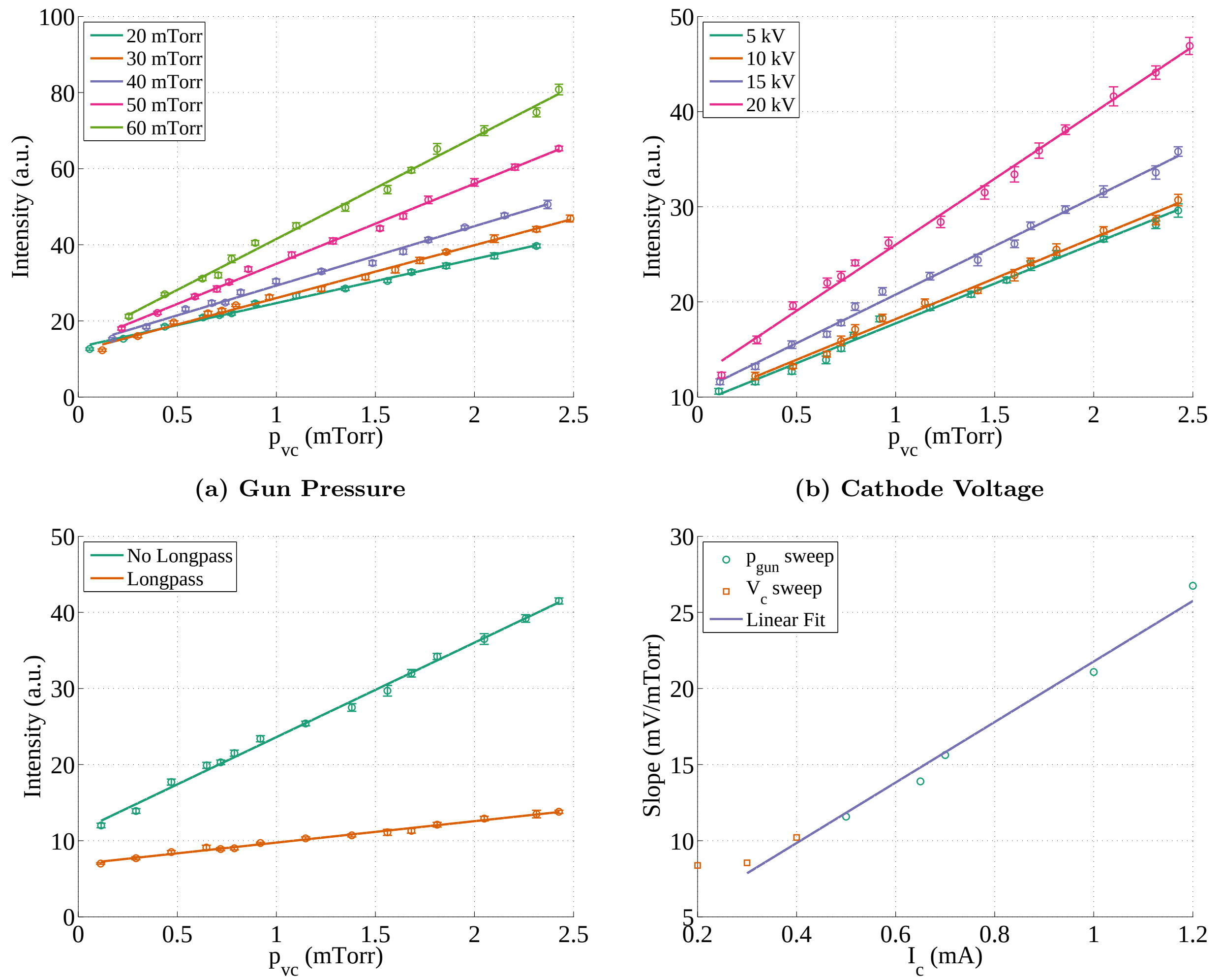

(a) Gun Pressure

(b) Cathode Voltage

(c) Longpass Filter

(d) Sensitivity

Figure 6. Effects of (a) WIPS chamber pressure, (b) cathode voltage, and (c) 725 nm longpass filter on the intensity of the PMT photocurrent. (d) Shows the slope of intensity vs pressure curve as a function of cathode current.Neutral gas was argon.

The measurement uncertainty was taken to be the average standard deviation of the 10 measurements.

From Fig. 6, it is observed that the PMT intensity scales linearly with the chamber pressure over the range of pressures tested, as anticipated from Eq. (2). From Fig. 6a, increasing the pressure in the gun is found to lead to an increase in emissions intensity for a given chamber fill pressure. In other words, the measurement system becomes more sensitive to changes in chamber pressure as the pressure in the electron gun is increased. Fig. 6b shows that the cathode voltage has a similar effect on the measured intensity, but only above a certain threshold voltage. Below ∼10 kV, the intensity appears to be unaffected by the cathode voltage. From 10 kV to 20 kV, however, the intensity at a given pressure is observed to increase with cathode voltage, indicating that increased cathode voltage also improves the sensitivity of the measurement system to changes in chamber pressure.

Fig. 6c indicates that while the intensity is significantly reduced by the presence of the longpass filter, suggesting that a substantial fraction of the collected light possesses a wavelength shorter than the 725 nm cutoff of the filter, the relationship between intensity and chamber pressure remains linear. It is currently unknown, however, whether the slope of intensity vs pressure response scales in the same manner as that of the total emissions.

By measuring the cathode current for each of the cases in Figs. 6a and 6b, the relationship between I_c and the slope of the intensity vs pressure response, i.e., the sensitivity of the diagnostic system, was established.

Fig. 6d shows that the slope scales linearly with cathode current over nearly the entire range of conditions tested. It is suspected, however, that at low V_c, the beam current no longer scales linearly with cathode voltage, and therefore the measurement sensitivity is not expected to scale linearly with cathode current. As such, the lowest voltage case ($V_c = 5\,\mathrm{kV}$) was excluded from the linear fit.

With this data point omitted, the line of best fit was found to have a slope of $19.9\,(\mathrm{mV/mTorr})\,/\mathrm{mA}$. If we ignore the non-zero y-intercepts, using the argument that they are small relative to the slopes, then this value is the sensitivity of the diagnostic system and can be used to give an estimate of the cathode current necessary to obtain a desired signal strength at a given chamber background pressure. For example, to obtain a $5\,\mathrm{mV}$ signal at the lower end of EP relevant pressures, $\sim 1 \times 10^{-6}$ Torr, we find that a cathode current of $I_c \approx 250\,\mathrm{mA}$ would be required.

Importantly, the observed linear trend is found to hold regardless of whether I_c was varied as the result of changes in gun pressure or cathode voltage. This supports the claim that the gun pressure and cathode voltage are primarily affecting the measurement sensitivity through the cathode current, rather than vice versa.

C. Comparison with Fast Ion Gauge

To examine how the TREBF measurement system compared to a known diagnostic, both the TREBF system and a fast ion gauge (FIG) were used to independently perform temporal measurements of the neutral density of argon gas rapidly puffed into the vacuum chamber. A Parker-Hannifin Series 9 miniature solenoid pulse valve was attached to the vacuum chamber and used to inject $10\,\mu$s pulses of argon at varying pressures. A comparison between the time-dependent FIG and TREBF neutral density measurements is shown in Fig. 7. The FIG indicates a sharp rise in neutral density occurring over a $\sim 0.5\,\mathrm{ms}$ timescale, followed by a gradual fall off. The smaller trailing peak occurring at $t \approx 6\,\mathrm{ms}$ is attributed to an unintended second puff of gas that is thought to result from incomplete sealing during the rapid shutoff of the puff valve. The mean and standard deviation of three different TREBF measurements is shown as the red shaded region in Fig. 7. It is clear that the TREBF measurement compares well with the FIG, most notably the time agreement of the first and second density peaks and the rate of decay from these peaks. Finally, an upper limit on the time response of the TREBF diagnostic system was estimated from the arrival of the neutral gas front to each measurement location. By fitting a curve of the form $A\,\exp(t/\tau)$ to data in the region near $t = 1\,\mathrm{ms}$, we obtain measured response times of $\tau_{FIG} = 60 \pm 10\,\mu$s and $\tau_{TREBF} = 70 \pm 10\,\mu$s. This analysis demonstrates the high-speed measurement capabilities of TREBF and suggests a temporal resolution of at least $70\,\mu$s. Given that the RC time of the measurement system was $t_{RC} \approx 50\,\mu$s, however, it is anticipated that the response time could be made much faster by the use of a high speed current to voltage conversion circuit.

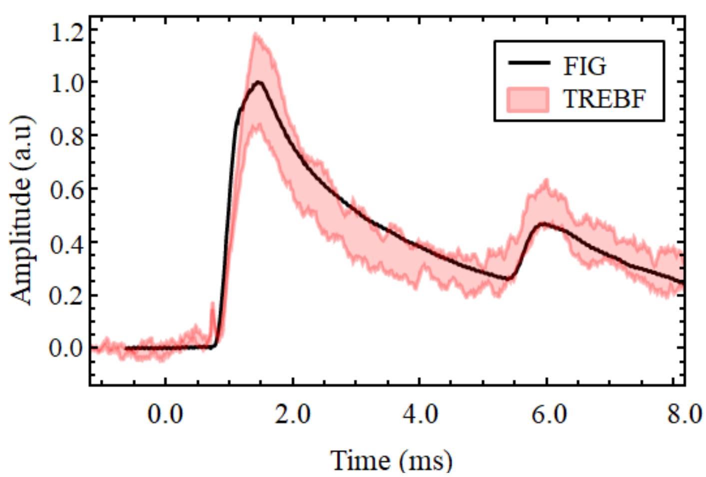

Figure 7. Comparison of EBF to FIG response for a $10\,\mu$s pulse of argon at 9.3 psig

.

D. Demonstration with Plasma Source

To obtain a more accurate estimate of the true time response of the TREBF system as well as gain a better understanding of how the system would perform in an EP relevant plasma environment, the TREBF system was used to measure the neutral refill time of an FRC thruster. For these tests, the PMT photocurrent was converted into a measurable voltage using a high speed transimpedance amplifier circuit based on the Texas Instruments OPA380 chip. This circuit allowed for a 1×10^5 V/A gain with a theoretical response time of $\lesssim 1\,\mu$s. Moreover, data was recorded on a LeCroy® data acquisition system (DAQ) using an 12 bit Jorger digitizer card, which allowed for the PMT measurements to be precisely synchronized with the plasma source. The PMT gain was set relatively low at 4×10^4 to prevent the voltage corresponding to the peak plasma intensity from exceeding the ± 5 V input voltage limit of the DAQ. In addition, a 830 nm center wavelength, 10 nm full width half max bandpass filter was used to collect primarily neutral argon emissions.

1. *Ungated*

Fig. 8 shows the timing of the plasma emissions relative to the flux through the two formation coils. The three major peaks observed in the PMT signal are found to correspond to the major zero crossings of the flux through the coils. These crossings occur at field reversal, the beginning of FRC ejection, and accelerator turn-off, respectively. Smaller peaks can be observed at the zero crossings caused by the ringing of the theta pinch. The ability of the PMT response to closely track the changes in flux indicates that the TREBF diagnostic has a response time on the order of a few microseconds or better, in agreement with theoretical estimates. As evidenced by Fig. 8, this temporal resolution allows TREBF to measure phenomena on time scales relevant to EP plasmas.

Fig. 9 shows the PMT signal as a function of time both when no electron beam is present as well as for electron beam cathode voltages of 7 kV and 14 kV. It should be noted that the data shown is the average of 10 shots taken in quick succession. It is observed that, at the relatively low gain and high chamber pressure at which the measurements were taken, the effect of the electron beam is minimal. While some differences between the three cases may be observed near the first two peaks, these regions were found to be areas of high shot-to-shot variation. Despite attempts to mitigate random variations by taking a 10 shot average, it cannot be claimed with confidence that the relatively small differences in the measured emissions are not simply due to random variations in the plasma that are unrelated to the presence of the electron beam.

The inset of Fig. 9 shows the emissions in the region well after the third peak. While small compared to the three major peaks, there appears to be a relatively long lived decay in the emissions over a period of approximately $100\,\mu$s some time after the third peak. It is hypothesized that this signal may be due to the fluorescence of neutral particles as they refill the formation section of the chamber. At the low gain setting, however, the signal during refill is difficult to distinguish from the background noise. A simple way

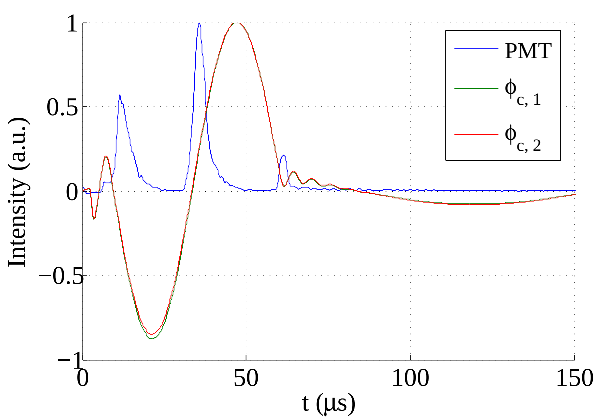

Figure 8. Timing of plasma emissions relative to the magnetic flux through the coils with no electron beam and for a chamber fill pressure of 1.7 mTorr.

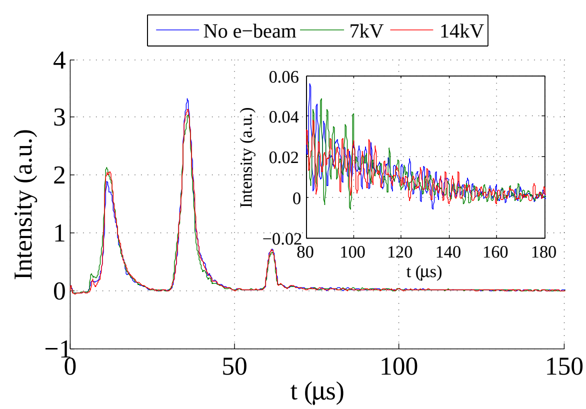

Figure 9. Effect of electron beam on plasma emissions measured using PMT with 830 nm bandpass filter. Fill pressure in the chamber was $p_{vc} = 1.7$ mTorr.

to improve the signal to noise ratio would be to increase the PMT gain. Since the signal in this region is orders of magnitude smaller than the peak values, however, simply increasing the gain would potentially cause the PMT to saturate and, moreover, would cause the measured voltage at peak intensity to be larger than the DAQ can handle. Thus before increasing the gain, it is necessary to implement some type of gating, such that the high intensity emissions from the formation process are blocked from entering the PMT.

2. Gated

To achieve PMT gating with microsecond scale resolution, a custom gate circuit based on the design of Iwata et al[19] was constructed. In this circuit, gating is achieved by controlling the voltage applied to two of the PMTs dynodes. When no control voltage is applied, two of the dynodes are reversed biased 50 V to 90 V below their normal values and the PMT is kept in a normally-off state. To switch the PMT on, a gate pulse is supplied to a high speed pulse generating circuit, which generates a voltage pulse that is applied to the dynodes and forward biases them to their normal values. While, in principle, any two dynodes could be controlled, Iwata et al[19] found that controlling the 2nd and 4th or 2nd and 5th dynodes typically yielded the best results.

Instead of the Thorlabs PMTSS module used in previous tests, a Hamamatsu R9110 PMT was used for testing the gating circuit so that the PMT dynodes could be directly accessed. The R9110 is a 9 stage, multialkali, side-on, circular cage type PMT with a sensitive spectral range of 185 nm to 900 nm. The maximum gain of this PMT was 1×10^8, although in the present configuration it is limited to 2×10^7, which was higher than the PMTSS and should therefore allow for ample amplification of the fluorescence signal. Fig. 10 compares the gated and ungated signal from the PMT when no electron beam was present. When ungated, the familiar triple peak structure appears, similar to Fig. 9. During gated operation, however, it was observed that the first two peaks are highly attenuated while the third peak, which occurs after the gate pulse, is unaffected, indicating successful gated operation. PMT gain control was also demonstrated, with a 1V increase in gain voltage resulting in an approximately sixfold increase in signal strength. In attempting to replicate the scaling results of Fig. 6a, however, it was found that the fluorescence of the background gas could not be detected using the gated PMT, even when no filters were used to attenuate the plasma emissions. Since the maximum gain of the R9110 PMT is comparable to or better than the PMTSS, it is unlikely that insufficient PMT gain was the cause. Possible explanations include that the optical system used to couple light into the PMT was not as optimized as it was for the previous measurements or that the custom gating circuit inexplicably did not allow for the full PMT gain to be realized.

The response time of the gated PMT for a variety of control voltages is shown in Fig. 11. It is found that the time response is decreased at larger gain control voltages. This relationship is hypothesized to be due to the effect of the increased charge voltages on the coupling capacitors used to gate the dynodes. It

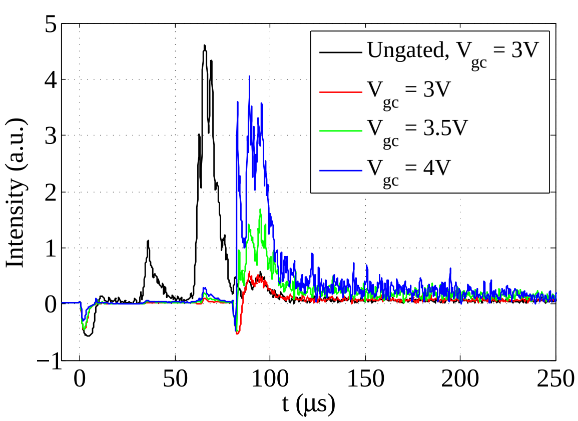

Figure 10. Demonstration of gated PMT operation at a fill pressure of $p = 0.9$ mTorr. The gate pulse was applied at $t = 80\,\mu$s and had a $300\,\mu$s width. An 830 nm bandpass filter was used to block broadband radiation.

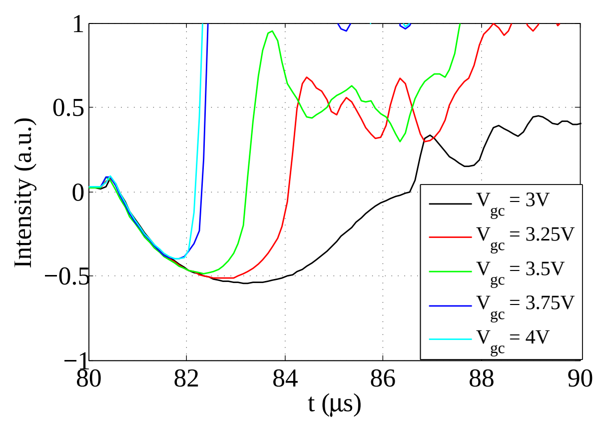

Figure 11. Typical time response of the gated PMT system. Response times of $\leq 10\,\mu$s were typical, with the turn-on time decreasing with increasing gain control voltage.

should be noted, however, that despite slight variations across gain settings, response times of $\leq 10\,\mu$s or better were achieved for all gain settings of interest. This level of response is thought to be sufficiently fast to capture the neutral refill phenomena, which is expected to occur on the timescale of 100s of microseconds to milliseconds.

In addition, attempts to measure the neutral refill were hindered by the relatively low background rejection ratio achieved by the gating circuit, which resulted in insufficient attenuation of the peak emissions at higher PMT gain settings. A background rejection ratio, defined as the ratio of the signal measured when the PMT gated on versus off, of approximately 8000 was achieved by Iwata et al[19] using the same circuit design and commercial gated PMTs typically achieve 10^4 or better. From Fig. 10, however, it was estimated that the rejection ratio achieved by our gating circuit and PMT combination was on the order of 1×10^2 to 1×10^3. This indicates that our prototype gated PMT could be significantly improved and suggests that rejection ratios high enough to block out the initial high intensity peaks should be attainable through refined circuit design.

V. Conclusion

A proof-of-concept experiment was constructed to test the feasibility of applying a relatively old hypersonic flow diagnostic technique, electron beam fluorescence, to the study of neutral particle dynamics in electric thrusters. An electron gun was created capable of delivering $\sim$100μA of beam current with a beam waist of $\sim$5 mm to a location up to $\sim$50 cm from the location of the gun. The collisional excitation of neutral particles and resulting fluorescence yielded a measurable signal at pressures down to 0.2 mTorr in argon. Comparison between the probe signal and fast-ion gauge for a fast puff of neutral gas showed excellent agreement. Finally, measuring the emission of plasma radiation from a pinch plasma it was determined that the optical detection system is capable of providing an overall time response of $\sim$1μs.

Further development of the TREBF diagnostic seeks the following improvements: (1) construction of a pulsed electron gun capable of $\sim$50 mA peak current, (2) improved understanding of beam propagation through thruster magnetic fields, (3) development of a collisional-radiative model incorporating plasma and electron beam excitation, and (4) system design for in-vacuum operation in an EP test environment.

Acknowledgments

The authors would like to thank Dr. Mike Kendra and Dr. Mitat Birkan, and acknowledge that the electron beam fluorescence diagnostic system was supported by AFOSR Contract Number FA9550-17-C-0009, and the theory, imaging, and optical filtering were supported by AFOSR Contract Number FA9550-17-1-0045.

This material is based upon work supported by the National Science Foundation Graduate Research Fellowship Program under Grant No. DGE-1256082. Any opinions, findings, and conclusions or recommendations expressed in this material are those of the authors and do not necessarily reflect the views of the National Science Foundation.

References

[1] Walker, M. L. and Gallimore, A. D., "Neutral density map of Hall thruster plume expansion in a vacuum chamber," *Review of Scientific Instruments*, Vol. 76, No. 5, 2005, pp. 053509.

[2] Crintea, D., Czarnetzki, U., Iordanova, S., Koleva, I., and Luggenhölscher, D., "Plasma diagnostics by optical emission spectroscopy on argon and comparison with Thomson scattering," *Journal of Physics D: Applied Physics*, Vol. 42, No. 4, 2009, pp. 045208.

[3] Hori, T., Bowden, M., Uchino, K., Muraoka, K., and Maeda, M., "Measurements of electron temperature, electron density, and neutral density in a radio-frequency inductively coupled plasma," *Journal of Vacuum Science & Technology A: Vacuum, Surfaces, and Films*, Vol. 14, No. 1, 1996, pp. 144–151.

[4] Crofton, M., Hsu Schouten, A., Young, J., Beiting, E., Diamant, K., Corey, R., and Delgado, J., "Neutral Xenon Density in the SPT-140 Near-Field Plume," *33rd International Electric Propulsion Conference, IEPC Paper*, Vol. 399, 2013, pp. 6–10.

[5] Aanesland, A., Liard, L., Leray, G., Jolly, J., and Chabert, P., "Direct measurements of neutral density depletion by two-photon absorption laser-induced fluorescence spectroscopy," *Applied Physics Letters*, Vol. 91, No. 12, 2007, pp. 121502.

[6] Crofton, M. W., "Measurement of neutral xenon density profile in an ion thruster plume," *AIAA Paper*, , No. 96-2290, 1996.

[7] Diop, B., Bonnet, J., Schmid, T., and Mohamed, A., "Compact Electron Gun Based on Secondary Emission Through

Ionic Bombardment," *Sensors*, Vol. 11, No. 5, 2011, pp. 5202–5214.

[8]Schilling, J., Pobst, J., and Erwin, D., "The Use of Pulsed Electron Beam Fluorescence for Arcjet Plume Diagnostics," *23rd International Electric Propulsion Conference*, 1993, pp. 93–130.

[9]Packan, D., Bonnet, J., and Rocca, S., "Number Density and Velocity Measurement in the Plume of a Micronewton Cold Gas Thruster by Electron Beam Fluorescence and Laser Induced Fluorescence," *31st International Electric Propulsion Conference*, 2009, pp. 2009–184.

[10]Jarrige, J., Packan, D., Duchemin, O., and Balika, L., "Assessment of the azimuthal homogeneity of the neutral gas in a hall effect thruster using electron beam fluorescence," *34th International Electric Propulsion Conference*, 2015, pp. 2015–394.

[11]Polzin, K. A. and Choueiri, E. Y., "Performance optimization criteria for pulsed inductive plasma acceleration," *IEEE transactions on plasma science*, Vol. 34, No. 3, 2006, pp. 945–953.

[12]Kirtley, D., Slough, J., Pfaff, M., and Pihl, C., "Steady operation of an electromagnetic plasmoid thruster," *8th MSS/5th LPS/5th SPS Joint Subcommittee Meeting*, 2011.

[13]Byers, D. and Dankanich, J. W., "A review of facility effects on Hall effect thrusters," *31st International Electric Propulsion Conference*, 2009, pp. 2009–076.

[14]Diamant, K. D., Liang, R., and Corey, R. L., "The effect of background pressure on SPT-100 Hall thruster performance," *AIAA Paper*, Vol. 3710, 2014.

[15]Randolph, T., Kim, V., Kaufman, H., Kozubsky, K., Zhurin, V., and Day, M., "Facility effects on stationary plasma thruster testing," *23rd International Electric Propulsion Conference*, 1993, pp. 13–16.

[16]Brown, D. L. and Gallimore, A. D., "Investigation of low discharge voltage hall thruster operating modes and ionization processes," Tech. rep., AIR FORCE RESEARCH LAB EDWARDS AFB CA PROPULSION DIRECTORATE, 2009.

[17]Gadamer, E. O., "Measurement of the density distribution in a rarefied gas flow using the fluorescence induced by a thin electron beam," Tech. rep., University of Toronto, 1962.

[18]Steinhauer, L. C., "Review of field-reversed configurations," *Physics of Plasmas*, Vol. 18, No. 7, 2011, pp. 070501.

[19]Iwata, T., Takasu, T., and Araki, T., "Simple photomultiplier tube internal-gating method for use in subnanosecond time-resolved spectroscopy," *Applied spectroscopy*, Vol. 57, No. 9, 2003, pp. 1145–1150.